



Analytical particle measurements in an optical microflume

Joseph D. Taylor, Alex Terray, Sean J. Hart*

Naval Research Laboratory, Chemistry Division, Bio/Analytical Chemistry Section, Code 6112 4555 Overlook Ave. S.W., Washington, DC 20375, USA

ARTICLE INFO

Article history:

Received 23 December 2009
Received in revised form 27 April 2010
Accepted 29 April 2010
Available online 7 May 2010

Keywords:

Optical chromatography
Laser
Pressure
Microfluidics
Optofluidic
Optical trapping
Pneumatics

ABSTRACT

In this work, microscopic particles in a fluid flow are manipulated using forces generated by a high power laser beam. The resulting manipulations on the particles are imaged using a microscope lens connected to a CCD camera. Differential forces on particles of varying physical and chemical composition have been measured. The goal is to measure the optical forces on a diverse range of particles and catalog the associated chemical and physical differences to understand which properties and mechanisms result in the largest force differentials. Using these measurements our aim is to better understand differences between similar microspheres in terms of size, morphology, or chemical composition. Particles of the same size, but different composition show large variations in optical pressure forces and are easily discernable in the present analytical system. In addition, we have demonstrated the ability to differentiate a 70 nm size difference between two NIST precision size standard polystyrene microspheres, corresponding to a 2.0 pN difference in optical force. Lastly, the instrument was used to measure differences between biological samples of similar size, demonstrating the ability to make precise analytical measurements on microorganism samples.

© 2010 Published by Elsevier B.V.

1. Introduction

The interaction between photons and microscopic particles induces optical pressure by imparting a fraction of their momentum when they scatter at the surface or refract through a particle. This effect is considerable when using a collimated light source such as a laser, given the remarkably high number of photons available. The more well-known optical micromanipulation technique known as optical tweezers utilizes a single highly focused laser for tasks such as trapping [1,2] and sorting cells [3,4], or a combination of laser beams working in unison for the development of unique non-intrusive tools such as microactuators [5,6]. The beams can be tightly focused into the solution that is transporting the microscopic particles through a microchip or flow cell. The translucent particles experience a net restoring force that traps them at the laser's focal point, a result of photon momentum transfer from the sharply converging light leaving a microscope objective. By either altering the aqueous environment or repositioning the laser beam, micron-sized particles can be maneuvered and manipulated in real-time in a highly controlled manner.

Abbreviations: OC, optical chromatography; PS, polystyrene; PMMA, poly(methylmethacrylate); Si, silica; MF, melamine formaldehyde resin; *Ba*, *Bacillus anthracis* (Sterne strain); *Bt*, *Bacillus thuringiensis*; Geobacter, *Geobacter sulfurreducens* (strain DL-1).

* Corresponding author. Tel.: +1 202 404 3361; fax: +1 202 404 8119.
E-mail address: sean.hart@nrl.navy.mil (S.J. Hart).

In a mildly focused laser beam, micron-sized particles experience a radiation pressure force in the direction of the laser propagation and towards regions of high intensity along the beam waist. Kim et al. recently devised a straightforward cross-type optical particle separator with broad applicability toward sorting and separating biological cells at constant velocity. A mixture of 5 and 10 μm particles flowing through a microchannel would encounter a mildly focused laser beam propagating perpendicular to the flow and would be deflected from their original path depending on their size [7,8]. Novel optical force switches also incorporating less divergent beams with longer depths-of-focus have been developed to sort mammalian cells in microfluidic chips by essentially pushing them laterally [9]. Conventional optical chromatography (OC) relies on this force when balanced against an opposing fluid flow [10]. In this case, the diverging portion of the laser beam (i.e. some distance from the focal point) is carefully aligned within and along a capillary separation channel in such a way as to direct the beam toward the approaching fluid carrying the incoming microparticles. When the optical pressure exerted on the particles equals the fluid drag force, particles become trapped within the beam in a stable manner and in unique positions along the beam axis. Particle positioning depends on size [11] and shape [12], but also arises due to differences in refractive index [13,14]. These larger size and/or greater refractive index particles encounter a pronounced optical pressure resulting in their being pushed further down the length of the beam and requiring less photon density relative to smaller or less refractive particles. Using this approach allows the unique separation and retention of various particles on the basis

Report Documentation Page

Form Approved
OMB No. 0704-0188

Public reporting burden for the collection of information is estimated to average 1 hour per response, including the time for reviewing instructions, searching existing data sources, gathering and maintaining the data needed, and completing and reviewing the collection of information. Send comments regarding this burden estimate or any other aspect of this collection of information, including suggestions for reducing this burden, to Washington Headquarters Services, Directorate for Information Operations and Reports, 1215 Jefferson Davis Highway, Suite 1204, Arlington VA 22202-4302. Respondents should be aware that notwithstanding any other provision of law, no person shall be subject to a penalty for failing to comply with a collection of information if it does not display a currently valid OMB control number.

1. REPORT DATE 2010	2. REPORT TYPE	3. DATES COVERED 00-00-2010 to 00-00-2010	
4. TITLE AND SUBTITLE Analytica Chimica Acta		5a. CONTRACT NUMBER	
		5b. GRANT NUMBER	
		5c. PROGRAM ELEMENT NUMBER	
6. AUTHOR(S)		5d. PROJECT NUMBER	
		5e. TASK NUMBER	
		5f. WORK UNIT NUMBER	
7. PERFORMING ORGANIZATION NAME(S) AND ADDRESS(ES) Naval Research Laboratory, Chemistry Division, Bio/Analytical Chemistry Section, Code 6112, 4555 Overlook Ave. S.W., Washington, DC, 20375		8. PERFORMING ORGANIZATION REPORT NUMBER	
9. SPONSORING/MONITORING AGENCY NAME(S) AND ADDRESS(ES)		10. SPONSOR/MONITOR'S ACRONYM(S)	
		11. SPONSOR/MONITOR'S REPORT NUMBER(S)	
12. DISTRIBUTION/AVAILABILITY STATEMENT Approved for public release; distribution unlimited			
13. SUPPLEMENTARY NOTES			
14. ABSTRACT In this work, microscopic particles in a fluid flow are manipulated using forces generated by a high power laser beam. The resulting manipulations on the particles are imaged using a microscope lens connected to a CCD camera. Differential forces on particles of varying physical and chemical composition have been measured. The goal is to measure the optical forces on a diverse range of particles and catalog the associated chemical and physical differences to understand which properties and mechanisms result in the largest force differentials. Using these measurements our aim is to better understand differences between similar microspheres in terms of size, morphology, or chemical composition. Particles of the same size, but different composition show large variations in optical pressure forces and are easily discernable in the present analytical system. In addition, we have demonstrated the ability to differentiate a 70 nm size difference between two NIST precision size standard polystyrene microspheres, corresponding to a 2.0pN difference in optical force. Lastly, the instrument was used to measure differences between biological samples of similar size, demonstrating the ability to make precise analytical measurements on microorganism samples.			
15. SUBJECT TERMS			
16. SECURITY CLASSIFICATION OF:			17. LIMITATION OF ABSTRACT Same as Report (SAR)
a. REPORT unclassified	b. ABSTRACT unclassified	c. THIS PAGE unclassified	
19a. NAME OF RESPONSIBLE PERSON			

of their intrinsic and/or extrinsic properties, from polymeric beads and silica-based spheres to biological particles such as pollen and pathogenic bacteria [15,16].

Accordingly, recent research concerning optical manipulation has attempted to understand the influence of composition on the optical pressure of particles under study, rather than merely a size-based dependence. Our group has recently demonstrated that microbiological separations can be achieved within a microfluidic device incorporating optical forces as a means to interrogate minute dissimilarities in a heterogeneous sample containing co-injected microbes [17]. In this particular case, two closely related genetic relatives, *Bacillus anthracis* and *Bacillus thuringiensis*, displayed large differences in their retention distances. This report and others [18] have provided keen insight into the separation of biological particles in a laminar flow system based on intrinsic physical and biological characteristics. Understanding these optofluidic force differentials may result in new avenues to separate biological species using a sorting methodology that exerts no physical contact on the material. Other reports have examined the influence of such intrinsic properties as refractive index by studying the laser-trapping properties in a controlled manner using synthetic microspheres of known refractive index [19].

Previously, optical chromatography research had demonstrated partial optical separation of a fraction of injected particles based upon size [11]. Our laboratory extended optical chromatography for size-independent separation of polymeric particles based on variations in refractive index [13]. Herein we demonstrate a novel analytical technique based upon optical chromatography for obtaining measurements of the optical force required to trap a particle at a set position within a microfluidic separation channel. Holding the laser power constant, a single particle may be retained at a pre-defined position within the channel by adjusting the flow rate, thus creating an optical microflume. Each particular particle becomes trapped with a unique and highly reproducible flow rate, which is used to calculate the fluidic drag force. Since the two opposing forces are balanced when the particle is stationary, the drag force equals the optical force acting on the particle. This approach has demonstrated the ability to easily differentiate between various polymeric and inorganic microbeads of the same size, as well as the ability to discern minute differences in size of particles of the same material (70 nm). To further demonstrate the instrument's capability, genetically similar biological samples of *B. anthracis* and *B. thuringiensis*, as well as wild-type *Geobacter sulfurreducens* bacterial cells have been analyzed.

2. Experimental

2.1. Materials

The primary materials studied consisted of two NIST traceable polystyrene (PS) precision size standard spheres (1.80 ± 0.04 , 1.90 ± 0.03 μm) as well as 1.97 μm PS, 1.98 μm poly(methylmethacrylate) (PMMA) microbeads, and 2.00 μm silica (Si) beads, which were all obtained from Polysciences (Warrington, PA, USA). The 2.03 μm melamine formaldehyde resin (MF) particles were from Corpuscular, Inc. (Cold Spring, NY, USA). Si, PMMA, PS, and MF have refractive indices of 1.43, 1.49, 1.59 and 1.68, respectively. Phosphate buffered saline $1\times$ (PBS) was from Invitrogen (Carlsbad, CA, USA) and was used as the carrier liquid for the biological samples. *B. anthracis* avirulent strain Sterne lacking the pXO2 plasmid was previously obtained from the Colorado Serum Company, Denver, Co. and *B. thuringiensis* serovar, *kurstaki* strain 4D7 was obtained from Bacillus Genetic Stock Center at The Ohio State University (Columbus, OH, USA). Sporulation and spore purification are described in detail in a previous report [17].

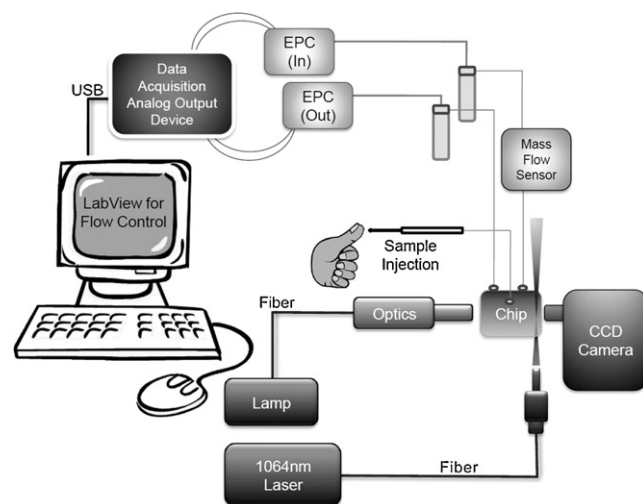


Fig. 1. System schematic showing electronic pressure controllers that control the inlet and outlet pressure in 20 mL vials for precise fluidic pumping. Flow is monitored through a CMOS mass flow meter anterior to the microchip. A near infrared laser is mildly focused using a 0.5 in. plano-convex 100 mm focal length lens into the analysis channel (55 μm) where the width of the beam expands to nearly fill the channel.

Wild-type *G. sulfurreducens*, strain DL-1 (Geobacter) bacterial cells produced with pili were provided by Dr. Bradley Ringeisen at the NRL (Code 6113).

2.2. Instrumentation

The primary components of the optical chromatography system illustrated in Fig. 1 consisted of a continuous wave (CW) 1064 nm ytterbium fiber laser (IPG Photonics, Oxford, MA, USA), an electronically controlled pneumatic pumping system governed by LabView (National Instruments, Austin, TX, USA), a liquid mass flow SLG1430 sensor (Sensirion, Staefa, Switzerland) coupled with nanofluidic connections and tubing from Upchurch Scientific (Oak Harbor, WA, USA), and a custom made microfluidic network with nanopore connections to an inlet, outlet and injection line [20]. The microchip was mounted onto a plexiglass plate fitted onto a 4-axis positioner, while the camera, PL-800 fiber optic illuminator (Edmund Optics, Barrington, NJ, USA), and laser fiber were each fitted to an x - y - z translation platform, all from Thorlabs (Newton, NJ, USA).

The optically transparent microfluidic flow cell had a liquid volume of approximately 500 nL. The chip was bonded together in a sandwich fashion using three fused silica plates with laser-etched channels and inlets as described in a previous report [21]. Imaging was performed using a Retiga 1300 12-bit cooled color CCD (QImaging, Surrey, BC, Canada) coupled with a $20\times$ microscope objective from Olympus (Center Valley, PA, USA) with a focused white light source behind the separation channel. Data were collected using ImagePro Plus 6.0 (Media Cybernetics, Bethesda, MD, USA) to measure the position of the optically trapped microparticles in the liquid flow. The diameter of the separation channel was 55 μm , while the length was 500 μm . The laser light was focused through a 0.5 in. diameter plano-convex 100 mm focal length lens and aligned such that the width of the beam filled the separation channel.

MilliQ water and/or PBS were pumped through the flow cell and precisely controlled using Pneutronics miniature electronic pressure controllers (EPC) from Parker-Hannifin (Cleveland, OH, USA) capable of delivering steady, pulse-free liquid flow using nitrogen gas. Each EPC controlling the gas directed over the "inlet" and "outlet" liquid reservoirs was regulated by a 4P4C breakout board with an R/A connector from Winford Engineering (Bay City, MI, USA),

each powered by a 3 W AC/DC to DC transformer with 24 V DC output from McMaster-Carr (Robbinsville, NJ, USA) and both controlled via a 16-bit, 8 channel high-drive data acquisition analog output device from Measurement Computing (Norton, MA, USA), which connects to a PC via a USB connection governed by custom written flow control software written in LabView.

3. Results and discussion

3.1. Instrumental design considerations and optimization

This manuscript describes the novel development of an optical chromatography separation device for use as a unique instrument to probe minute size differences, physical attributes and variations in the chemical composition of micron-sized particles. This has been accomplished partially due to the development of a pneumatic pumping system that replaces conventional syringe-based pumping systems, allowing precise control of the flow in order to make highly reproducible measurements. By carefully pressurizing an inlet and outlet vial with an inert gas such as nitrogen, electronic pressure controllers (EPCs) provide an avenue to control the flow in order to distinguish particles of the same size having different refractive indices, as well as particles that are very similar in size. By taking all of the measurements on the various microparticles at a fixed location within a flow channel and holding the laser power constant for the various samples studied, simply altering and measuring the flow rate provides a unique and convenient way to calculate the fluidic drag force on the particles in order to correlate these values to differences in optical force. This is accomplished by solving for the fluid drag force in laminar flow which is governed by Stokes' law:

$$F = 6\pi\eta a v$$

where F is the drag force, η is the fluid's dynamic viscosity, a is the radius of the particle, and v is the linear velocity derived from the fluid flow rate through the microchannel. When the particle traveling through the microchannel encounters the laser beam, the particle comes to rest at an equilibrium point where the optical and drag forces are equal.

In order to accurately calculate these forces, stable flow with precise control is essential. Fig. 2 shows flow rate (nLmin^{-1}) versus time (s) for both the pneumatic system and a low-flow-rate syringe pump, which clearly demonstrates the advantages of the pneumatic flow system. Relative to syringe-based pumping, the pneumatic system provides immediate response to altering the flow rate; there are no syringe-size limitations as the vials used have a 20 mL capacity; switching from infuse to withdraw is both effortless and instantaneous; and the flow is remarkably stable for

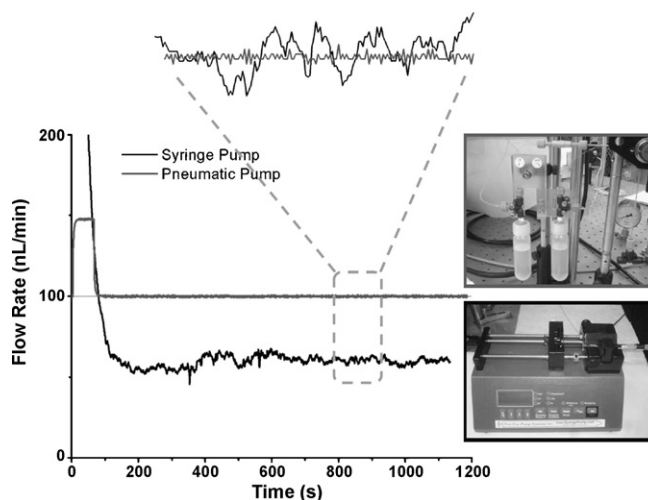


Fig. 2. Comparison of a low-flow-rate syringe pump using a 1-mL glass syringe with the pneumatic electronically controlled pumping system used herein. The magnified region is normalized to show the precision of the flow when compared to the “most stable” region from the syringe pump. RSD values for this region are 2.3% and 0.3% for the syringe pump and pneumatic pumping system, respectively.

an indefinite period of time. On the other hand, syringe pumps may take several minutes to stabilize after a change in flow rate, are limited to the size of syringe that may be used (1 mL in this case), may not dispense at the rate at which they are actually set, and show large instability in both the short and long term. A quantitative comparison of the flow rates between the syringe pump and the pneumatic pumping system at the magnified region of the graph (the flattest portion of the curve for the syringe pump) demonstrates RSD values of 2.3% and 0.3%, respectively. It should be noted that the flow sensor reads the measured flow velocity with a noise level of $\pm 0.5 \text{ nLmin}^{-1}$ immediately prior to entering the microfluidic flow cell.

Contrary to previous setups, the flow cell depicted in Fig. 3A was assembled such that the separation channel was aligned in a vertical position in order for the laser to enter from the bottom of the channel and trap incoming particles flowing down toward the beam. The benefit of this arrangement relative to the separation channel fixed in a horizontal position was to avoid gravity pulling trapped particles across the width of the beam, as well as across the parabolic flow profile of the transporting solution. Once a particle is trapped in the channel, minute lateral movements of the translation platform housing the laser optics enabled us to essentially outline the parabolic flow profile. To demonstrate the capability of the design, several well-known and often-used particles of known

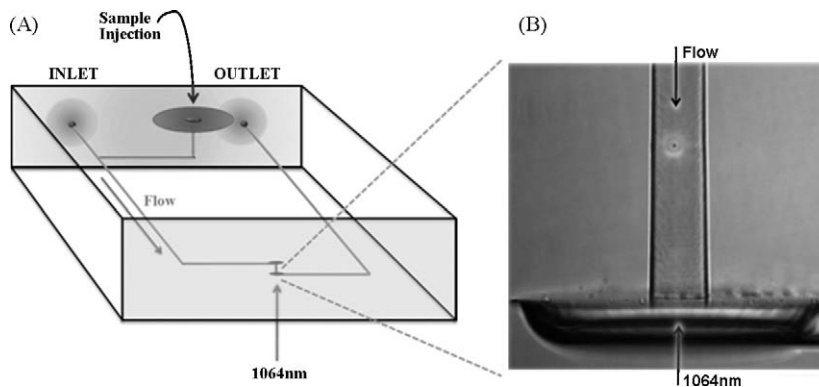


Fig. 3. (A) 3D schematic of the glass microfluidic chip and separation channel. (B) CCD camera image of a $1.97 \mu\text{m}$ polystyrene microparticle balanced against opposing fluidic and optical forces.

Table 1

Data representing the instrument's ability to analyze particles by chemical composition, size, and its application in differentiating biological particles. Force is presented in pN calculated from Stokes' viscous drag expression, including a prolate spheroid model for biological particles. N represents the number of trials performed, each of which consisted of a 30-image sequence at a rate of one image per second. Conditions: 2.6 W laser power, 1064 nm.

	Size (μm)	Trials (N)	Flow rate (nL min^{-1})	Optical force (pN)
Si	2.00	11	19.2 ± 3.1	2.4
PMMA	1.98	10	40.5 ± 2.8	5.0
PS	1.97	10	96.2 ± 3.6	11.8
MF	2.03	10	112.9 ± 5.5	14.3
PS (1.80)	1.80 ± 0.04	10	71.7 ± 3.4	8.1
PS (1.90)	1.90 ± 0.03	10	82.8 ± 3.0	9.8
<i>Ba</i>	1.28×0.71	13	55.6 ± 5.1	3.5
<i>Bt</i>	1.72×0.75	10	38.3 ± 4.2	2.8
<i>Geobacter</i>	1.5×0.5	5	21.3 ± 0.6	1.1

refractive index were employed and trapped at the peak of the empirically derived flow profile, which was near the center of the microchannel. Given the nature of the device, the highest achievable flow rate using the pneumatic pumping arrangement was approximately 150 nL min^{-1} . As such, it was imperative to find an optimal laser power at which all particles could be suitably trapped at their respective flow rates. The 1064 nm laser used was held constant at the empirically determined power of 2.6 W throughout the duration of the experiments.

3.2. Optical force differentiation based on refractive index

Initial studies incorporated various types of microparticles all approximately $2.0 \mu\text{m}$ in size. These consisted of polystyrene (PS), poly(methylmethacrylate) (PMMA), silica (Si), and melamine formaldehyde resin (MF). PS was initially injected into the system by filling a $250 \mu\text{L}$ Hamilton syringe with a low concentration of particles in ultrapure water and connecting the tapered steel tip to a tubing sheath connected to 100 microns i.d., 360 microns o.d. tubing leading to the injection port on the flow cell. Immediately prior to the particles encountering the separation channel, they reach a broadened opening where the particles decelerate and may be pinned against the wall with relative ease [20–22]. At this point, although the beam has diverged and the photon density is significantly lower, particles may be retained and collected and individually released by temporarily blocking the laser beam. PS was used prior to collecting data and was used as a daily calibration standard to ensure that the particles could be reproducibly trapped at the same position within the channel at the same flow rate. Fig. 3B shows a PS particle retained in the separation channel at the pre-defined location.

Table 1 contains data comparing the various samples studied and the flow rates at which they are optically retained. All measurements were taken approximately $125 \mu\text{m}$ from the focal point of the laser beam. The fluid drag force required to trap and hold the different types of particles is consistent with the refractive index of each particle, with the more refractive particles trapping at higher flow rates than the less refractive particles that are retained at relatively low flow rates. These flow rates can be correlated to linear velocity and incorporated into Stokes' viscous drag equation, as the low speed and non-turbulent flow (i.e. low Reynolds number) allow for calculation of the force. When solving the expression for force, the viscosity of the transporting solution must be incorporated, while accounting for absorptive heating from the laser [23]. Every watt of laser power corresponds to an approximately 3.5°C increase from room temperature (22°C) [21]. From observing these

minute differences in optical force, this instrument has demonstrated its analytical feasibility to readily differentiate particles of known composition in a highly reproducible fashion independent of size.

3.3. Calibration and error assessment

Each particle type behaves differently in the retention region. Si has the lowest refractive index and most closely resembles a biological cell, thus is less well retained while being analyzed. MF on the other hand is nearly motionless, even at relatively high flow rates, and also has the highest refractive index. To properly account for any variation above or below the arbitrary position in the microchannel where all of the measurements were made, particles were studied as a function of flow rate to their positions in the analysis region. Fig. 4 shows linear correlations that were obtained for each particle type in order to make corrections to particle movement. A particle's vertical position around the analysis zone (represented by the y-axis) was altered by arbitrarily changing the flow rate both up and down, and a series of 50 images collected and averaged at each position. Error bars are depicted in both the vertical and horizontal direction, which demonstrates the reproducibility of obtaining precise flow readings between measurements. From these linear curves, the data in Table 1 were obtained by performing particle tracking analysis on each 30-image raw data sequence (10 or 11 sequences total per particle) using the particle tracking function in ImagePro 6.0. Any deviation in the vertical direction (i.e. y-axis) above or below the analysis zone in the channel could be converted from a distance in pixels to a distance in micrometers, and correlated to the flow rate from the curve. If the assumption is made that the particle is perfectly stationary at the set point, the uncorrected standard deviations were shown to be off by factors of 19.6, 16.0, 10.7, and 12.7 for PS, PMMA, Si, and MF, respectively.

3.4. Optical force differentiation based on size and cell type

Although size-based separations are quite prevalent, our goal was to study the possibility of differentiating minute differences in size of the same material and the applicability of the technique to biological samples. Initially, three sizes of polystyrene, 1.80, 1.90 and $1.97 \mu\text{m}$, were tested to further probe the efficiency of the device. From the data included in Table 1 the device can differentiate as small as a $0.07 \mu\text{m}$ (70 nm) difference in size, which corresponds to a difference in optical force of 2.0 pN. An estimate of the best size discrimination possible for particles around the $1.80 \mu\text{m}$ diameter range (using 3.4 nL min^{-1} full error obtained from experiment) indicates that particles differing by only 41 nm should be easily discernable. If further optimization can be made in the instrumentation, it may be possible to probe even smaller differences on the surface of any number of particles and particle types, including biological samples. Extending this work to include biological colloids has been a key motivating directive for work in this area [24,25]. To prove this initial capability, two genetically similar spore samples, *B. anthracis* (*Ba*) and *B. thuringiensis* (*Bt*), were measured. These have been thoroughly characterized in a previous report [17]. These spores exhibit nearly identical refractive indices, and have relatively similar widths ($Ba = 0.71 \mu\text{m}$, $Bt = 0.75 \mu\text{m}$). However, *Bt* is slightly longer ($Ba = 1.28 \mu\text{m}$, $Bt = 1.72 \mu\text{m}$) and its exosporium tends to be larger, whereas the exosporium on *Ba* tightly surrounds the spore proper. The lower refractive index cells were less well retained in the analysis region at 2.6 W. Higher laser power was necessary in order to capture the cells and perform single measurements. Data in Table 1 shows that the two spores were trapped at unique flow rates, thus demonstrating the ability of the analytical device

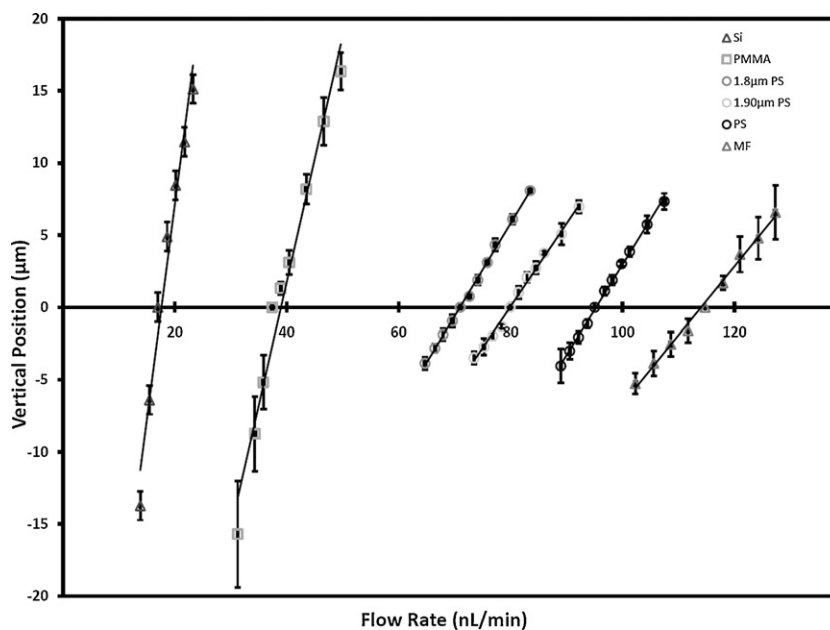


Fig. 4. Linear correlation data for each particle type. Error bars represent triplicate measurements with both horizontal and vertical error bars (error along the x-axis is smaller than the size of the objects). $Y=0$ corresponds to the arbitrary position in the microchannel where all of the measurements were taken. Conditions: 2.6W laser power, 1064 nm.

to probe these small variations at higher laser power (5 W). We tested one more cellular sample, generously provided to us by the Ringeisen lab, consisting of *Geobacter proteobacteria* which are often used in microbial fuel cell studies [26] and are a particularly useful tool for bioremediation [27]. These pill-shaped cells exhibit a fur-like coating of microbial nanowires known as pili, and have approximate cell body dimensions of $1.5\ \mu\text{m}$ in length by $0.5\ \mu\text{m}$ in width. In order to properly determine the fluid drag force on these non-spherical biological particles, the equation used must be modified. Thus, the expression used determines the fluid drag force in relation to a prolate spheroid, which is given by:

$$F = 6\pi\eta b\nu K$$

where K is a correction to Stokes' law that takes into account both the polar radius or long axis, a , and the equatorial radius or short axis, b , of the prolate spheroid [28]. This sample was also differentiable from the spore samples and is included in Table 1, thus providing a promising lead to the instrument's ability to study more biological samples. For future applications, our group has recently designed a new microfluidic chip incorporating a microchannel width that is approximately five times that of the chip used in this work. The larger dimensions are amenable for the measurement of larger biological particles and in cellular studies where particles in the $5\text{--}25\ \mu\text{m}$ size range can be analyzed without considerable back pressure in the channel and alleviating any affinity the particles may encounter with the channel walls when in close proximity.

4. Conclusion

We have developed a unique method for probing minute size differences among particles of the same chemical composition, as well as made several analytical comparisons among similarly sized particles of differing composition. This work builds upon previous optical chromatography research to provide an analytical basis for evaluating various samples. With the ability to probe differences in size as small as 70 nm, the possibilities of other samples that may be interrogated are great. For more complex biological sam-

ples larger than a few micrometers, new microfluidic designs will be necessary to avoid negative pressure effects inside the analysis channel. As an analytical instrument, the approach can be readily extended to many samples in order to provide a starting point for comparison and help predict how samples in future work may trap relative to the unique properties or constituents of the microparticle.

Acknowledgements

The authors would like to acknowledge the Office of Naval Research and the Naval Research Laboratory for support of this research. Joseph D. Taylor is supported as an ASEE-NRL Postdoctoral Fellow.

References

- [1] A. Ashkin, J.M. Dziedzic, J.E. Bjorkholm, S. Chu, *Opt. Lett.* 11 (1986) 288–290.
- [2] J.R. Moffitt, Y.R. Chemla, S.B. Smith, C. Bustamante, *Annu. Rev. Biochem.* 77 (2008) 205–228.
- [3] T.N. Buican, M.J. Smyth, H.A. Crissman, G.C. Salzman, C.C. Stewart, J.C. Martin, *Appl. Opt.* 26 (1987) 5311–5316.
- [4] J. Oakey, J. Allely, D.W.M. Marr, *Biotechnol. Prog.* 18 (2002) 1439–1442.
- [5] R.C. Gauthier, M. Ashman, A. Frangioudakis, H. Mende, S. Ma, *Appl. Opt.* 38 (1999) 4850–4860.
- [6] D.G. Grier, *Nature* 424 (2003) 21–27.
- [7] S.B. Kim, S.Y. Yoon, H.J. Sung, S.S. Kim, *Anal. Chem.* 80 (2008) 2628–2630.
- [8] S.B. Kim, S.Y. Yoon, H.J. Sung, S.S. Kim, *Anal. Chem.* 80 (2008) 6023–6028.
- [9] M.M. Wang, E. Tu, D.E. Raymond, J.M. Yang, H. Zhang, N. Hagen, B. Dees, E.M. Mercer, A.H. Forster, I. Kariv, P.J. Marchand, W.F. Butler, *Nat. Biotechnol.* 23 (2005) 83–87.
- [10] T. Imasaka, Y. Kawabata, T. Kaneta, Y. Ishidzu, *Anal. Chem.* 67 (1995) 1763–1765.
- [11] T. Kaneta, Y. Ishidzu, N. Mishima, T. Imasaka, *Anal. Chem.* 69 (1997) 2701–2710.
- [12] R.C. Gauthier, M. Ashman, C.P. Grover, *Appl. Opt.* 38 (1999) 4861–4869.
- [13] S.J. Hart, A.V. Terray, *Appl. Phys. Lett.* 83 (2003) 5316–5318.
- [14] M.P. MacDonald, G.C. Spalding, K. Dholakia, *Nature* 426 (2003) 421–424.
- [15] S.J. Hart, A. Terray, K.A. Kuhn, J. Arnold, T.A. Leski, *Am. Lab.* 36 (2004) 13–17.
- [16] A. Terray, J. Arnold, S.J. Hart, *Opt. Express* 13 (2005) 10406–10415.
- [17] S.J. Hart, A. Terray, T.A. Leski, J. Arnold, R. Stroud, *Anal. Chem.* 78 (2006) 3221–3225.
- [18] M.P. MacDonald, S. Neale, L. Paterson, A. Richies, K. Dholakia, G.C. Spalding, *J. Biol. Regul. Homeost. Agents* 18 (2004) 200–205.
- [19] R.C. Gauthier, *Appl. Opt.* 41 (2002) 7135–7144.
- [20] S.J. Hart, A.V. Terray, J. Arnold, *Appl. Phys. Lett.* 91 (2007) 171121–171123.

- [21] A. Terray, H.D. Ladouceur, M. Hammond, S.J. Hart, *Opt. Express* 17 (2009) 2024–2032.
- [22] S.J. Hart, A. Terray, J. Arnold, T.A. Leski, *Opt. Express* 15 (2007) 2724–2731.
- [23] S. Ebert, K. Travis, B. Lincoln, J. Guck, *Opt. Express* 15 (2007) 15493–15499.
- [24] J. Harris, G. McConnell, *Opt. Express* 16 (2008) 14036–14043.
- [25] H. Zhang, K.K. Liu, *J. R. Soc. Interface* 5 (2008) 671–690.
- [26] H. Yi, K.P. Nevin, B.C. Kim, A.E. Franks, A. Klimes, L.M. Tender, D.R. Lovley, *Biosens. Bioelectron.* 24 (2009) 3498–3503.
- [27] D.R. Lovley, *Nat. Rev. Microbiol.* 1 (2003) 35–44.
- [28] J. Happel, H. Brenner, *Low Reynolds Number Hydrodynamics with Special Application to Particulate Media*, Martinus Nijhoff Publishers, Boston, 1983, pp. 154–156.